Journal of Materials Chemistry A

Accepted Manuscript

ROYAL SOCIETY OF CHEMISTRY

www.rsc.org/materialsA

Journal Name

ARTICLE

Modification of epoxy resin through the self-assembly of a surfactant like multi-element flame retardant

Received 00th January 20xx,
Accepted 00th January 20xx

DOI: 10.1039/x0xx00000x

www.rsc.org/

C. Liu, T. Chen, C. H. Yuan, C. F. Song, Y. Chang, G. R. Chen, Y. T. Xu and L. Z. Dai*

In order to develop a multi-element synergistic flame retardant system, the combination of DOPO, POM and POSS was achieved by using the classical Kabachnik-Fields reaction. The as designed POSS-bisDOPO was characterized by FT-IR, ^{1}H NMR, ^{13}C NMR, ^{31}P NMR, 2D NMR, and MS. POSS-bisDOPO was introduced into epoxy resins to obtain flame retardant materials. The LOI value can reach up to 34.5% with a 20 wt% content of POSS-bisDOPO. TGA results showed that the char yield could be significant improved in cured POSS-bisDOPO/EP. The ATR-FTIR, optical images and SEM analyses indicated that the residual char had a compact and coherent appearance in inner layer, while the outer sider structure was intumescent and multi-porous. Therefore, by isolating heat and oxygen more efficiently, the char played an important role in improving the excellent thermal stability and flame retardancy of cured POSS-bisDOPO/EP. The three point bending test results showed that the mechanical strength of the POSS-bisDOPO/EP was higher than that of pure EP and POSS-NH_2/EP, owning to the outstanding reinforced effect from the unique nano-structure of POSS-bisDOPO assembled in EP matrix. These data indicated that POSS-bisDOPO could not only obviously enhance the flame retardancy, but also improve the mechanical properties of epoxy resins.

Introduction

Epoxy resins have already gained wide applications in microelectronics packaging materials, surface coating, adhesive and advanced composite matrices, owing to their excellent moisture, solvent and chemical resistances, low shrinkage on cure, toughness, strong adherence to many substrates, good mechanical and dielectric properties[1-3]. Nonetheless, like many other normal polymers, the main shortage of epoxy resins is flammability. Halogens (particularly Cl and Br) have been widely used to improve the flame retardancy of epoxy resins over several decades. However, the use of halogen-containing flame retardant additives are evoking the environment issue as they would produce poisonous substance such as hydrogen bromide, dibenzo-*p*-dioxinand dibenzo-furan during combustion[4]. Therefore, it is highly desirable to develop halogen-free flame retardant to improve burning resistance of epoxy resins. Phosphorus, nitrogen and silicon become the favoured elements due to their excellent flame retardance.

Polyhedral oligomericsilsesquioxane (POSS) and 9, 10-dihydro-9-oxa-10-phosphaphenanthrene-10-oxide (DOPO) are typical silicon-containing and phosphorus-containing flame retardants, respectively, both of which can significantly reduce the flammability and increase char yields of polymeric materials[5-10]. More importantly, additives simultaneously containing silicon and phosphorus can achieve synergistic flame-retardant effect[11-14], thus increasing the flame retardance more effectively. For instance, Mu *et al.*[15] reported a phosphorus-containing polyimide-POSS nanocomposites which can protect the underlying material from atomic oxygen by forming highly effective self-passivating layers. Unlike simply adding these two kinds of flame retardant in the polymer matrix, Yang *et al.*[11, 16, 17] synthesized a flame retardant (DOPO-POSS) by chemically connecting phosphorus and silicon moieties. It was an effective flame retardant additives for epoxy resin, polycarbonate and polyamide. In the study of Wang *et al.*[12], two novel phosphorus-nitrogen-silicon flame retardants were introduced into cycloaliphatic epoxy. A dense and compact graphitized layer composed of silicon was formed, thus preventing the materials from burning.

However, most current flame retardants containing silicon/phosphorus reported in literatures were obtained by relatively complex synthetic route, and a lower yield as well. Herein, we modified POSS with DOPO through an efficient "one-pot" Kabachnik-Fields reaction[18, 19] to afford a surfactant like multielement flame retardant (POSS-bisDOPO). Nano flame-retardant materials were constructed by the self-assembly of POSS-bisDOPO in epoxy resin. The structure of POSS-bisDOPO as well as the morphology, flame retardant properties and mechanical properties of POSS-bisDOPO/EP systems were investigated in details by using FT-IR, NMR, MS, LOI, SEM, TGA, DSC and three point bending techniques, respectively.

Fujian Provincial Key Laboratory of Fire Retardant Materials, College of Materials, Xiamen University, Xiamen 361005, People's Republic of China.
E-mail: lzdai@xmu.edu.cn.

Electronic Supplementary Information (ESI) available: Additional experimental details and spectra, including a schematic diagram for proposed mechanism of the synthesis of POSS-bisDOPO, ^{13} C, 2D NMR and MS spectra of POSS-bisDOPO, a figure indicating thermogravimetric measurements of POSS-bisDOPO (air atmosphere, 10 °C min^{-1}), and a figure indicating thermogravimetric measurements of control samples (air atmosphere, 10 °C min^{-1}).
See DOI: 10.1039/x0xx00000x

Results and discussion

Synthesis and Structure Characterizations

POSS-bisDOPO was synthesized *via* Kabachnik-Fields reaction[18] among $-NH_2$ in POSS-NH_2, HCHO and P-H in DOPO (Scheme 1a). Its chemical structure was confirmed by FT-IR spectroscopy, ^1H, ^{13}C, ^{31}P, ^1H-^1H COSY and ^1H-^{13}C HMQC NMR spectroscopy, and mass spectroscopy. The FT-IR spectra of POSS-NH_2, DOPO, and POSS-bisDOPO are shown in Figure 1. In Figure 1d, the absorption peak around 2437 cm^{-1} which is attributed to P-H bond in DOPO disappears in POSS-bisDOPO. Nevertheless, several absorption peaks at 1640 cm^{-1}, 1225 cm^{-1} and 910 cm^{-1} corresponding to the aromatic ring, P=O and P-O-C of DOPO, as well as the peaks at 1090 cm^{-1} assigned to the Si-O-Si of POSS-NH_2, still exist in the spectrum of POSS-bisDOPO. However, the absorption peak of N-H in POSS-NH_2 was not obvious[20, 21]. In order to confirm the purity of this chemical reagent, we tested the mass spectrum of POSS-NH_2. As shown in Figure S3a in Supplementary Information, the molecular weight is as respected.

^1H NMR, ^{31}PNMR, ^{13}C NMR, ^1H ^1H COSY and ^1H ^{13}C HMQC NMR spectra of the resultant product are displayed in Figure 1, S1 and S2. All the protons can be attributed to the expected signals. Compared with the ^1H NMR spectra of the two original materials, the signal of P-H at 8.83 ppm in DOPO (Figure 1b) disappears and the new signals at 3.21 ppm and 3.69 ppm for the POSS-bisDOPO (Figure 1c) are assigned to methylene protons (i and i') in N-CH_2-DOPO group. In the ^{31}P NMR spectra, POSS-bisDOPO displays two signals at 32.2 and 32.34 ppm, while DOPO itself only has one characteristic signal at 14.71 ppm. The split of phosphorus signal in the ^{31}P NMR of POSS-bisDOPO is resulted from the steric hindrance of the two large volume DOPO pendant which leads to stereoisomer with unequal phosphorus.

Result of ESI-MS analysis for the POSS-bisDOPO is shown in S3b. Molecular ions identified is corresponding to the ionization with Na^+. It is verified that the final product of the POSS-bisDOPO is a single pure substance. All the results suggest that POSS-bisDOPO has been successfully synthesized through the one-pot three-component method with high purity and yield.

The thermal stability of POSS-bisDOPO was measured by TGA under air and nitrogen atmosphere respectively. As shown in Figure S4 and Table 2, POSS-bisDOPO has good thermal stability in air atmosphere, the temperature of 5 wt% weight loss is 333 °C, and its thermal degradation progress is classified into three steps. The maximum weight loss rate is about 0.21 wt%/min, and the residue char at 800 °C is 52.6%.

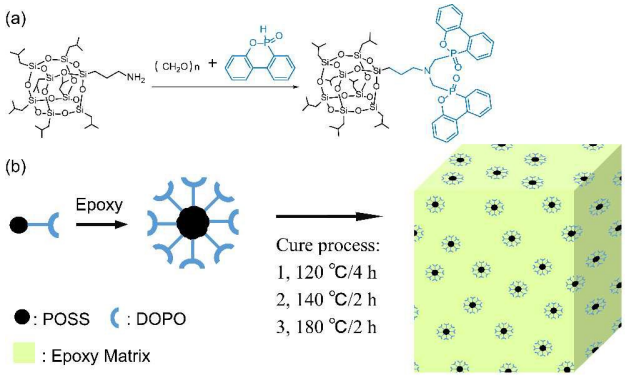

Scheme 1. Synthesic route of POSS-bisDOPO (a) and schematic illustration of the preparation process of POSS-bisDOPO modified epoxy resin (b).

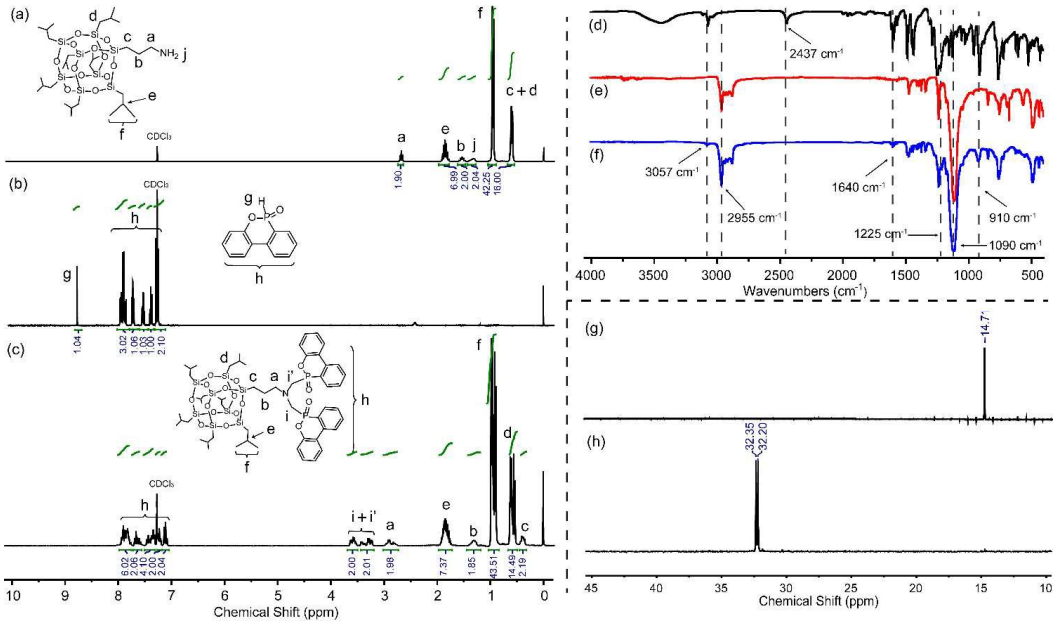

Figure 1. The ^1H NMR, FT-IR and ^{31}P NMR spectra of POSS-NH_2 (a, e), DOPO (b, d, g) and POSS-bisDOPO (c, f, h).

Self-assembly of POSS-bisDOPO in cured epoxy resins

DOPO has a high affinity to DGEBA, but the affinity of POSS-NH_2 in DGEBA is poor. The incorporation of DOPO onto POSS can dramatically enhance the compatibility of POSS-bisDOPO in DGEBA. However, the solubility of POSS-bisDOPO in DGEBA is still poor. Therefore, POSS-bisDOPO can self-assemble in DGEBA to form small particles, which is similar to the self-assembly behavior of a surfactant in water. Actually, aggregation of POSS-bisDOPO can be observed in the photographs shown in Figure 2. The transparency of the samples with POSS-bisDOPO (from EP-1 to EP-4) is lower than that of EP-0 and EP-DOPO. Moreover, the higher content of POSS-bisDOPO induces a lower transparency. Contrarily the EP-POSS is almost completely opaque, and the transparency of EP-(P+D) is between them. These results indicate that the compatibility of POSS-NH_2 in DGEBA is improved when it is modified by DOPO. This is possibly because DOPO has the similar benzene ring structure as DGEBA.

SEM images of the fracture were taken to further understand the micro morphology of cured epoxy nanocomposites. As shown in Figure 3, SEM images of samples before etching with DCM are different from those of the samples after etching. It can be seen that a lot of nanovoids are uniformly dispersed on the fracture surface, and the average size of the nanocavities is approximately 70 nm (inset in Figure 3 a'-d') which is far smaller than the wavelength of visible light (390-770 nm). This result further confirms the visual observation of transparency. In comparison, no nanovoids can be observed on the surface of samples without etching (inset in Figure 3 a-d). Notably, on the fracture surface of EP-POSS and EP-(P+D) (Figure S6), some uniform aggregates were observed in the continuous epoxy matrix, the particle size distribution was wide and the surface became rough. After etching by $CHCl_2$, the aggregates were replaced by holes (inset in Figure S6). On the surface of EP-(P+D) (Figure S6), there also have some aggregates, but less than that of EP-POSS. Because the compatibility of DOPO in DGEBA is much higher than that of POSS, we consider that POSS- bisDOPO can self-assemble into nanostructure with a

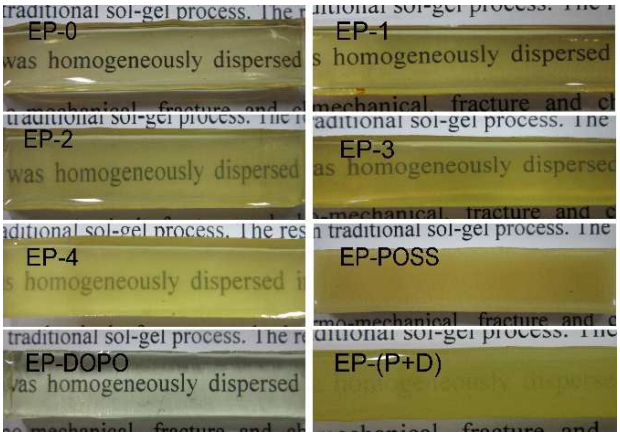

Figure 2. The photographs of cured epoxy resin and its nanocomposites.

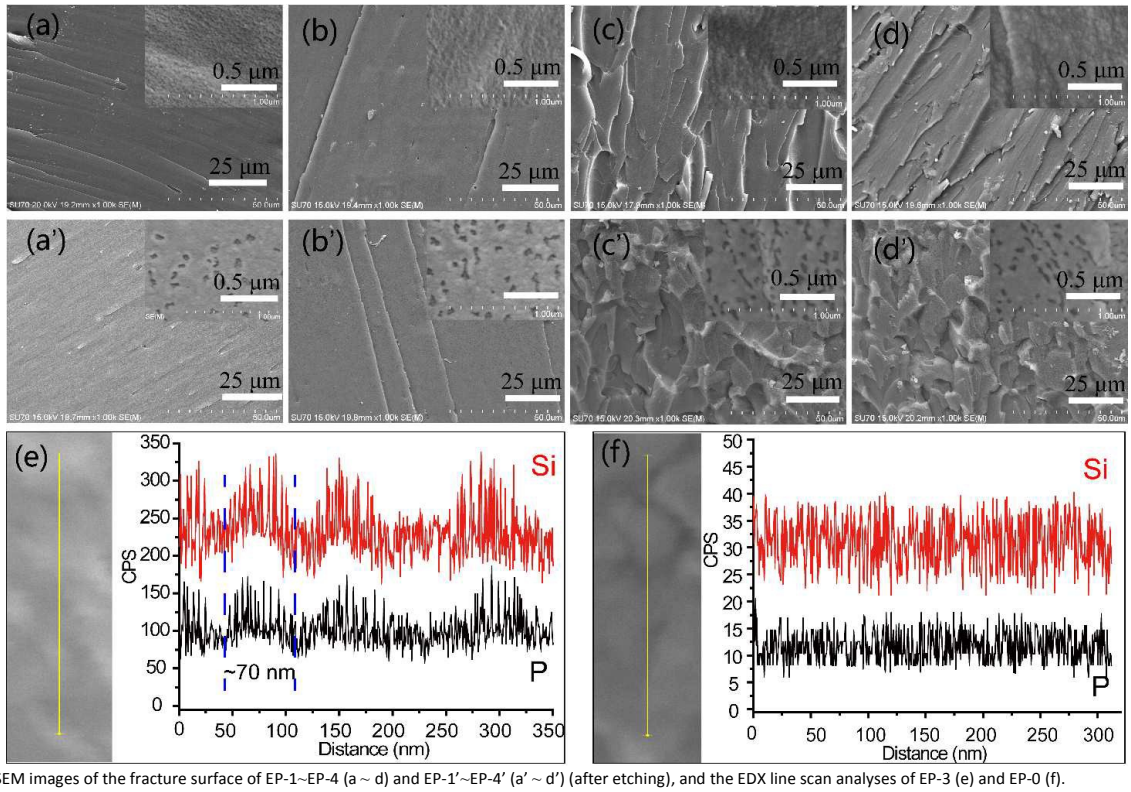

Figure 3. SEM images of the fracture surface of EP-1~EP-4 (a ~ d) and EP-1'~EP-4' (a' ~ d') (after etching), and the EDX line scan analyses of EP-3 (e) and EP-0 (f).

POSS core and a DOPO shell in the epoxy matrix (Schematic illustration is shown in Scheme 1). This self-assembly behaviour can significantly improve the dispersion of POSS component in DGEBA. .

To further judge the self-assembly behavior of POSS-bisDOPO in DGEBA, we performed the EDX line scan analysis of the samples without etching (Figure 3e and 3f). If the self-assembly the POSS-bisDOPO indeed exist in DGEBA, both Si and P elements should be enriched in nanoscaled domains instead of homogeneous dispersion. The EDX line scan analysis of Si and P elements for EP-3 is shown in Figure 3e. Evidently, both Si and P elements are enriched in nanoscaled domains, and the size of these domains corresponds well with that of the nanocavities in the etched samples. In comparison, EP-0 without POSS-bisDOPO shows much lower intensity of P and Si, and no element aggregation in the EDX line scan analysis (Figure 3f). This result provides a further indication for the self-assembly of POSS-bisDOPO in DGEBA.

Thermal properties characterization of cured epoxy and its nanocomposites

The glass transition temperature (T_g) is an important parameter that determines the application of epoxy resin thermosets. Figure 4 shows the DSC thermograms. Table 1 summarizes the sample compositions, flame retardant elements content, as thermosets display a higher T_g (≥145 °C) in comparison with the well as the T_g of the final materials. It is noteworthy that all the conventional epoxy thermosets reported in the literature[22, 23]. It is known that glass transition is generally ascribed to the segmental motion of the polymeric networks, and the T_g is determined by the degree of freedom for the segmental motion, crosslinking and entanglement constraints, and the packing density of the segments[24, 25]. The lower T_g value of the samples can be explained by the increasing of the packing density of POSS-bisDOPO.

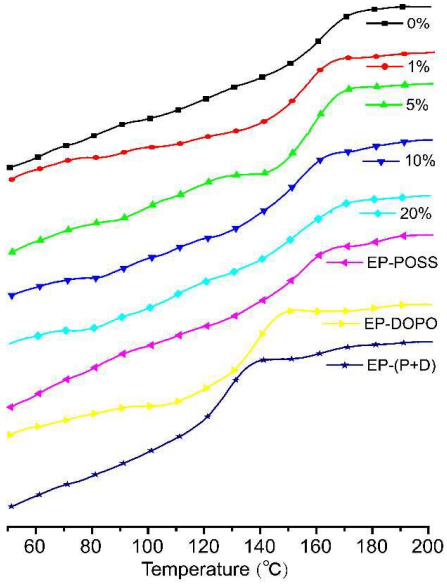

Figure 4. The DSC curves of cured epoxy resin and its nanocomposites.

Table 1. The compositions and T_g of cured epoxy resin and its nanocomposites.

Samples	DGEBA (wt%)	POSS-bisDOPO (wt%)	Element Content (wt%)		T_g
			P	Si	DSC
POSS-bisDOPO	-	-	4.6	16.8	-
EP-0	100	0	0	0	161.2
EP-1	99	1	0.05	0.17	154.4
EP-2	95	5	0.23	0.81	154.5
EP-3	90	10	0.46	1.68	153.6
EP-4	80	20	0.92	3.36	152.3
EP-POSS	95.2	5%POSS	0	0.81	153.8
EP-DOPO	95.2	5%DOPO	0.22	0	126.4
EP-(P+D)	95	1.67%DOPO, 3.33%POSS	0.23	0.81	127.4

The thermal stabilities of cured epoxy resin and its nanocomposites were investigated by TGA under air and nitrogen atmosphere, respectively. Figure 5 and S5 show the TGA and DTG curves. The initial decomposition temperature which is defined as the temperature of about 5 wt% weight loss (T_5), the temperature of maximum weight loss rate (T_{max}), and char yield at 800 °C are summarized in Table 2. All the samples have a single-step degradation progress under nitrogen atmosphere (Figure 5a and 5b) but have a two-step degradation progress under air atmosphere (Figure 5c and 5d), which are consistent with the results reported in literatures [26]. Under nitrogen atmosphere condition, T_5 and T_{max} of EP-0 are around 358 °C and 386 °C, and its maximum weight loss rate is 1.36 wt%·min^{-1}. However, the T_5 and T_{max} of EP-1 are about 345 °C and 384 °C, and the maximum weight loss rate is 1.26 wt.%·min^{-1}. The T_{max} decreased gradually with the increased POSS-bisDOPO content, the major reason of which can be attributed to the relatively low temperature for phosphorus

group degradation (mainly caused by the weak P-O-C bond decomposition in POSS-bisDOPO). This phenomenon was also observed in other phosphorus-containing epoxy resins[27]. However, increasing the POSS-bisDOPO content can gradually increase the residual char at 800 °C. Moreover, the maximum weight loss rate is decreased gradually when more POSS-bisDOPO is introduced into the epoxy matrix. These results indicate that higher char yield and slower degradation rate of nanocpmposites can be achieved by using more POSS-bisDOPO. Under air atmosphere condition, the first decomposition progress of all samples occurred at around 300 °C, implying that these samples adopt the same thermal decomposition pathway. This is probably induced by the dehydrogenation and aromatization of alkyl occurred at this temperature[28]. The second decomposition step occurred at around 570 °C, which can be attributed to the further degradation of the char layer[29]. Similarly, the residue char rate is increased and degradation rate is slowed down with the increasing POSS-bisDOPO load. Overall, TGA results reveal that POSS-bisDOPO can enhance flame retardancy by increasing the char yield and reducing the degradation rate.

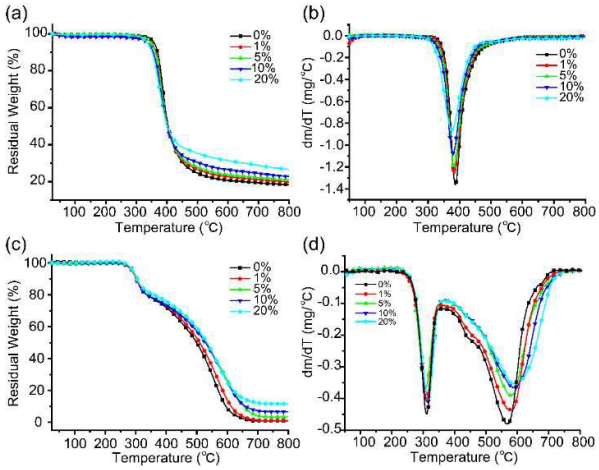

Figure 5. TGA and DTG curves of the cured neat epoxy and its nanocomposites with different loadings of POSS-bisDOPO ((a, b) nitrogen atmosphere, (c, d) air atmosphere, 10 °C min^{-1}).

Table 2. Thermal decomposition data for POSS-bisDOPO and its nanocomposites.

Samples	Nitrogen			Air			
	T_d	T_{max1}	Char	T_d	T_{max1}	T_{max2}	Char
POSS-bisDOPO	302.96	369.96	4.27	332.94	433.94	501.94	52.6
EP-0	355.43	384.43	18.40	290.05	304.05	559.05	0.91
EP-1	344.84	383..84	20.56	282.09	303.09	572.09	1.15
EP-2	347.75	381.75	21.05	290.93	308.93	574.93	3.39
EP-3	337.69	379.69	22.85	290.11	307.11	579.11	6.59
EP-4	337.71	374.71	26.59	289.84	300.84	582.84	11.53
EP-POSS	345.21	379.21	21.87	281.84	305.84	570.84	1.41
EP-DOPO	334.87	378.87	19.05	276.29	302.29	574.29	1.15
EP-(P+D)	343.67	380.67	19.95	281.05	303.05	562.95	2.93

In order to further investigate the degradation behaviour, FT-IR analysis was employed to confirm the change of chemical structure during the thermal oxidative process of neat EP and EP-4. The residues char which obtained from the thermal degradation under several representative temperatures (such as R.T., 200 °C, 300 °C, 400 °C, 500 °C, 600 °C and 800°C) were tested by FT-IR. Figure 6b shows the IR spectra of the residues char during the thermal degradation progress of EP-4, and by contrast, the IR spectra of the residues char of EP-0 were also studied (Figure6a). As shown in Figure 6a, the relative intensities of CH_2 stretching vibration at 2860-2948 cm^{-1} decrease gradually at 200 °C, and disappear completely over 300 °C, indicating the decomposition of hydrocarbon. It is worth noting that the peaks at 1607 cm^{-1}, 1507 cm^{-1}, 826 cm^{-1}, 750 cm^{-1} still exist at a high temperature region (≥400 °C), implying the formation of aromatic structures during pyrolysis process[30]. This is consistent with the TGA results. As shown in Figure 6b, the spectra are similar to that of neat EP, but a strong peak at 1090 cm^{-1} which assigned to the stretching vibration bond of Si-O-Si and P-O-P structures can be observed[31-33]. These results implied that the char residues of nanocomposites mainly comprise of Si-O-Si, P-O-P and aromatic structures, which function as a protective barrier that separates heat and cuts off oxygen.

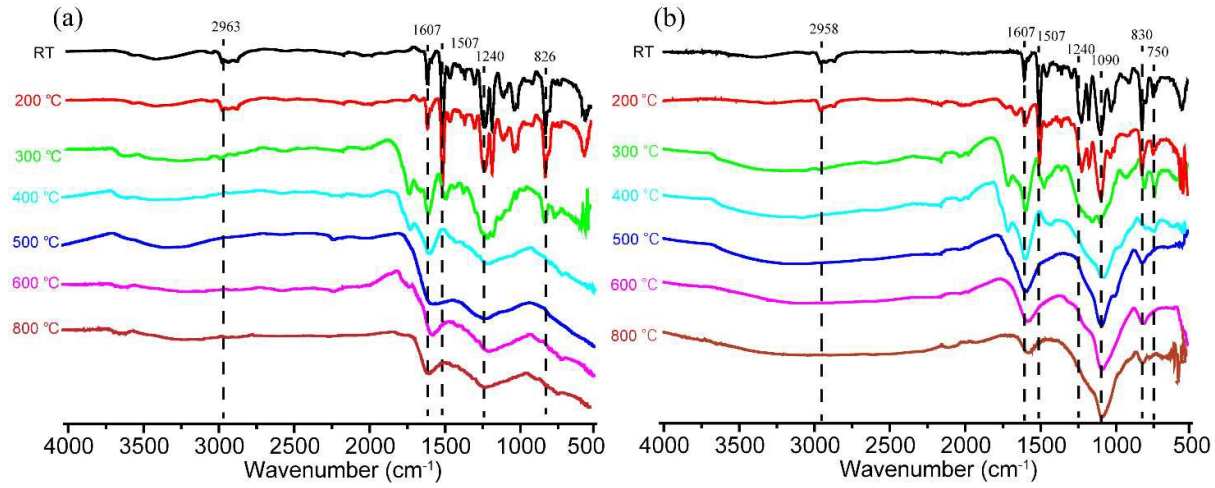

Figure 6. FTIR spectra of EP-0 (a) and EP-4 (b) at different pyrolysis temperatures.

Flame retardancy analysis of cured epoxy resin and its nanocomposites

The effect of POSS-bisDOPO on the flame resistance of cured epoxy resins was evaluated by LOI. As shown in Figure 7, the LOI value increased gradually from 25.4% to 34.5% with the increasing content of POSS-bisDOPO from 0 to 20 wt%. The LOI value of EP-POSS is lower than that of EP-DOPO, revealing that DOPO has a better flame resistance than POSS-NH_2. Moreover, the sample EP-(P+D) which has the same P and Si contents with EP-2 shows a lower LOI value (29.2%) than EP-2 (the LOI value is 31.7%). All these results demonstrate that POSS-bisDOPO can significantly improve the fire resistance of epoxy resins.

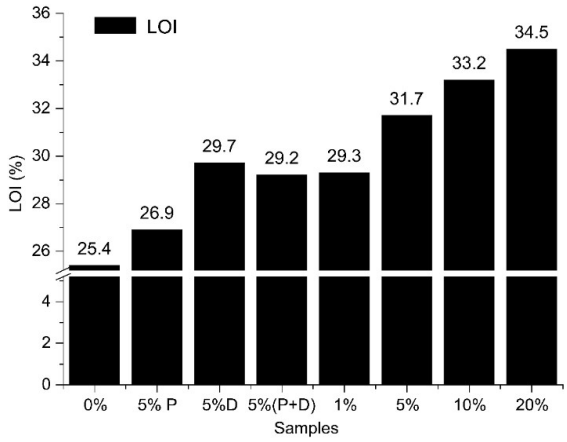

Figure 7. The LOI value of cured epoxy resin and its nanocomposites.

Figure 8a and b show the photographs of the EP-0 and EP-4 after maintaining at 800 °C for 30 min in a muffle furnace. The shape of EP-4 was still preserved after treating at 800 °C (Figure 8b), but the shape of the EP-0 was obviously destroyed (Figure 8a). The corresponding SEM images are shown in Figure 8 (c-f). The residue of EP-0 has obvious surface cracks (Figure 8c), which cannot act as a heat or oxygen shield to protect the inner matrix. Contrarily, the exterior char of EP-4 presents intumescent and multi-porous features (Figure 8d), and the inside of chars show a smooth and compact surface (Figure 8f). The difference between the inner and the outer surface can be observed more directly from the SEM image of the cross-section (Figure 8e). The smooth and compact structural feature of the char serves as an effective barrier against heat and oxygen diffusion and protect the polymer matrix inside from further burning. Whereas, the intumescent and multi-porous structure which fill with air could shield interior matrix from heat and protect the interior matrix from further combustion. The FT-IR spectra of nanocomposites and its residual char are shown in Figure 9. The peaks at 1090 cm^{-1} assigned to Si-O-Si and P-O-P bonds increased as the increasing addition of POSS-bisDOPO. The peaks appeared at around 1607, 1507, 826, and 750 cm^{-1} correspond to aromatic structures. After pyrolysis, the infrared characteristic peak of Si-O-Si and aromatic structures still could find in FT-IR spectra (shown in Figure 9b). This results also demonstrate that the heat and oxygen shield was mainly consist of Si-O-Si and aromatic structures.

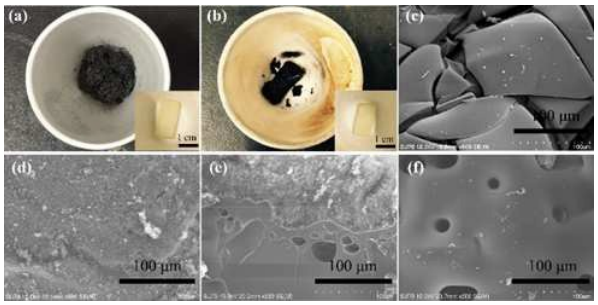

Figure 8. Photographs of EP-0 (a) and EP-4 (b), SEM images of the char EP-0 (c) and EP-4 (exterior (d), cross-section (e) and interior (f)).

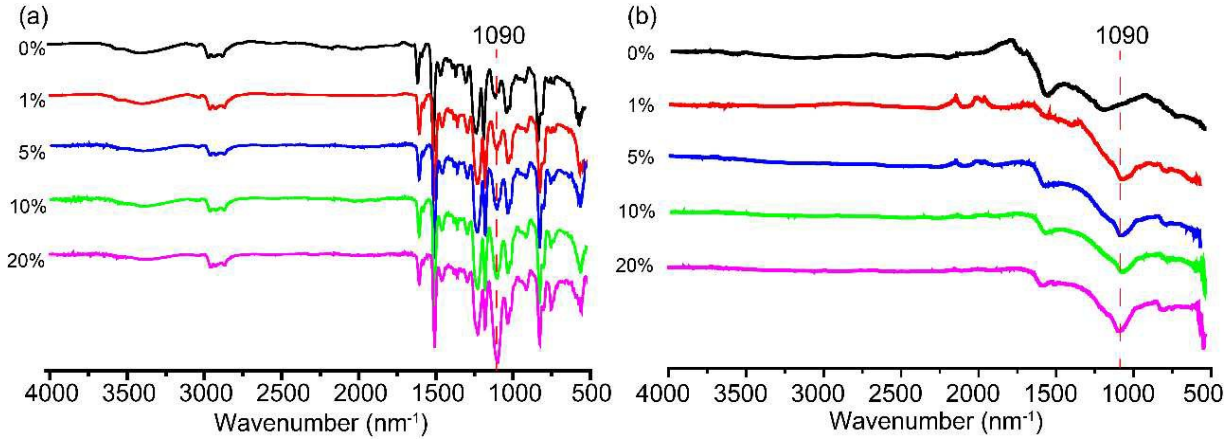

Figure 9. FTIR spectra of nanocomposites (a) and char residues (b)

To this end, we think that the mechanism of POSS-bisDOPO flame retardant epoxy resin is a condensed phase flame retardant pathway through charring and intumescence due to the synergistic between phosphorus, nitrogen and silicon. The char layer of the hierarchical structure can slowdown the heat and mass transfer, thereby protecting the underlying materials from further burning. The formation of char layer of hierarchical structure should be an important factor to achieve a better flame retardancy.

Mechanical property of cured epoxy resin and its nanocomposites

Finally, we are interested in demonstrating the influence of the nano-flame retardant on mechanical property of the nanocomposites. The three point bending test was used to measure the flexural strength of the nanocomposites systems. The flexural strength of a series samples bars with 5 wt% of POSS-NH_2, DOPO, P+D (1.67% DOPO, 3.33% POSS) and with an increasing mass fraction of POSS-bisDOPO (from 0 wt% to 20 wt%) are shown in Table 3. It can be observed that the flexural strength value of nanocomposites with POSS-bisDOPO are higher than EP-0, and reach the maximum value of 155.8 N/mm^2 at 10 wt% of POSS-bisDOPO. But a further increase of POSS-bisDOPO content led to a reduction of the strength. The higher strength of the samples at a lower POSS-bisDOPO content may be attributed to the formation of unique POSS-bisDOPO nanostructure in DEGBA, which acts as effective physical cross-link point. However, the POSS-bisDOPO assemblies aggregate in DGEBA when the POSS-bisDOPO concentration is too high. Thus, microscopic phase separation phenomena between POSS-bisDOPO and the EP matrix occurs, and the flexural strength tends to decrease. Also, decrease in flexural strength can be observed for EP-POSS (101.527 N/mm^2) and EP-DOPO (134.903 N/mm^2), in comparison with net EP (135.071 N/mm^2). Although EP-(P+D) has same content of POSS and DOPO with EP-2, but its flexural strength is lower than that of EP-2 (the flexural strengths is lowered by 25.49% than EP-2).

Table 3. The flexural strengths of cured epoxy resin and its nanocomposites.

Systems	Flexural strength (N/mm^2)	Percentage of increased flexural strength (%)
EP-0	135.071	0
EP-1	139.137	3.01
EP-2	142.846	5.76
EP-3	155.818	15.36
EP-4	150.881	11.70
EP-DOPO	134.903	-0.12
EP-POSS	101.527	-24.83
EP-(P+D)	106.434	-21.2

Experimental

Materials

Aminopropylisobutyl POSS, (Product No. AM0265) was purchased from Hybrid Plastics Company and used as received. 9, 10-dihydro-oxa-10-phosphaphenanthrene-10-oxide (DOPO) was purchased from Shanghai Eutec Chemical, China. Digycidyl ether of bisphenol A (DGEBA, trade name was E51) was a kind of liquid epoxy resins and supplied by Wuxi Resin Factory, China. 4, 4'-diaminodiphenylmethane (DDM) and polyoxymethylene (POM) were purchased from Sinopharm Chemical Reagent Co. Ltd., China. The reagents were used of analytical grade unless otherwise noted.

Synthesis of POSS-bisDOPO

POSS-NH_2 (50 mmol, 43.7 g), POM (125 mmol, 3.7 g), DOPO (125 mmol, 27.0 g) and chloroform (300 mL) were introduced into a 1000 mL round bottom glass flask equipped with a condenser and magnetic stirrer. The mixture was vigorously

stirred at 50 °C for 12 h. Then the solvent was concentrated to 50 mL by vacuum-rotary evaporation, followed by droped in 1000 mL of cold methanol slowly. The white precipitate was formed, and isolated by filtration and then dried under vacuum at 50 °C for 24 h, to give the title compound (POSS-bisDOPO, yield 61.3 g, 92.4%) as a white powder. The synthetic scheme of POSS-bisDOPO is shown in Scheme 1.

FTIR (ATR, cm^{-1}, Figure 1): 3057 (biphenyl in DOPO), 2860-2948 (C-H), 1640 (P-biphenyl), 1225 (P=O), 1090 (Si-O-Si, P-O-P), 910 (P-O-biphenyl); The NMR spectra of POSS-bisDOPO are shown in Figure 2, ^{1}H NMR ($CDCl_3$, 300 MH*z*) δ (ppm): 7.91 (2H, O-C-C<u>H</u>), 7.88 (2H, O-C-C-C<u>H</u>), 7.83 (2H, P-C-C<u>H</u>), 7.67 (2H, P-C-CH-CH-C<u>H</u>), 7.44 (2H, P-C-CH-C<u>H</u>), 7.35 (2H, P-C-C-C<u>H</u>), 7.24 (2H, O-C-CH-C<u>H</u>), 7.12 (2H, O-C-CH-CH-C<u>H</u>), 3.21-3.69 (4H, N-($C\underline{H}_2$-P)$_2$), 2.28-2.99 (2H, N-$C\underline{H}_2$-CH_2-CH_2-Si), 1.72-1.97 (7H, Si-CH_2-C<u>H</u>(-CH_3)$_2$), 1.23-1.40 (2H, Si-CH_2-$C\underline{H}_2$-CH_2-N), 0.83-1.04 (42H, Si-CH_2-CH(-$C\underline{H}_3$)$_2$), 0.51-0.68 (14H, Si-$C\underline{H}_2$-CH(-CH_3)$_2$), 0.34-0.47 (2H, Si-$C\underline{H}_2$-CH_2-CH_2-N); ^{13}C NMR ($CDCl_3$, 75 MHz) δ (ppm): 149.00 (2C, O-<u>C</u>), 135.42 (1C, P-C-<u>C</u>), 133.11 (2C, P-C-C-CH-<u>C</u>H), 130.96 (2C, P-C-<u>C</u>H), 130.45 (2C, P-C-C-<u>C</u>H), 128.30 (2C, P-C-CH-<u>C</u>H), 125.07 (2C, O-C-C-<u>C</u>H), 124.51 (2C, O-C-CH-<u>C</u>H), 123.51 (2C, O-C-<u>C</u>H), 122.98 (2C, O-C-<u>C</u>), 121.92 (2C, P-<u>C</u>), 120.34 (2C, O-C-C-CH-<u>C</u>H), 60.30 (1C, N-$\underline{C}H_2$-CH_2-CH_2-Si), 51.92 and 53.31 (2C, N-($\underline{C}H_2$-P)$_2$), 25.73 (14C, Si-CH_2-CH(-$\underline{C}H_3$)$_2$), 23.79 (7C, Si-CH_2-<u>C</u>H(-CH_3)$_2$), 22.46 (7C, Si-$\underline{C}H_2$-CH(-CH_3)$_2$), 20.16 (1C, Si-CH_2-$\underline{C}H_2$-CH_2-N), 9.17 (1C, Si-$\underline{C}H_2$-CH_2-CH_2-N); ^{31}P NMR ($CDCl_3$, 121 MH*z*) δ (ppm): 32.20 and 32.34 (DOPO); ESI-MS (40 eV) *m/z*: Calculated for POSS-bisDOPO = 1355.93 and Found. = 1355.9 $[M + Na]^+$. Anal. Calcd for $C_{57}H_{89}NO_{16}P_2Si_8$: C, 51.44; H, 6.74; N, 1.05%. Found: C, 50.85; H, 6.825; N, 0.972%. The stucture of POSS-bisDOPO was confirmed by ATR-FTIR, NMR and ESI-MS spectroscopy. These results confirmed that the target product was synthesized successfully.

Preparation of POSS-bisDOPO/E51/DDM thermosets and control samples

The flame retardant epoxy resins were obtained *via* thermally curing of DGEBA. POSS-bisDOPO and stoichiometric amounts of DDM were used as curing agents. The content of POSS-bisDOPO was 1 wt%, 5 wt%, 10 wt% and 20 wt%, and the resultant samples were marked as EP-1 to EP-4, respectively. The E51/DDM system without POSS-bisDOPO was used for preparing control sample 1 (marked as EP-0), and the E51/DDM sample only with POSS-NH_2 (5 wt%) was used for preparing control sample 2 (EP-POSS). Control sample 3 (EP-DOPO) was prepared by using only 5 wt% of DOPO. Control samples 4 (EP-(P+D)) was prepared by using 1.67 wt% of POSS and 3.33 wt% of DOPO to reach the same Si and P contents as the sample EP-2. To prepare these samples, E51 and flame retardant additive were mixed at 90 °C with continuously stirring until the mixture become transparent and then DDM was added into the mixture. The mixture were poured into aluminum mold once the mixture became homogeneous. A three-step curing procedure was carried out to obtain the thermosetting resins. All samples were programmed thermally curing at 120 °C for 4 h, followed by 140 °C for 2 h, and further postcured at 180 °C for 2 h to ensure the complete curing reaction. Thereafter, all the specimens were naturally cooled to room temperature from 180 °C in order to avoid stress cracking.

Characterization

Attenuated total reflectance Fourier transform infrared (ATR-FTIR) spectra were obtained on a Nicolet Avatar 360 spectrophotometer. Nuclear magnetic resonance (^{1}H NMR, ^{13}C NMR, ^{31}P NMR, ^{1}H ^{1}H COSY NMR and, ^{1}H ^{13}C HMQC NMR) spectra were recorded on a Bruker Advanced II AV300 MHz NMR spectrometer with $CDCl_3$ as the solvent. Mass spectrum (MS) were recorded by using an Esquire 3000 plus type mass spectrometer (Bruker Daltonics). Elemental (C, H, N) analyses were performed on a Vario EL III element analyzer.

Scanning electron microscope (SEM) images were obtained by using a SU-70. The morphological structure of fracture surfaces of the specimens before and after etching by DCM and the morphological structures of the char residue from LOI tests were observed. EDX line scan analysis of element was recorded at an accelerating voltage of 5 kV in order to reduce the interference that of the inner elements.

Thermogravimetric analysis (TGA) was performed with a Netzsch STA 409EP, heating from R.T. to 800°C at a heating rate of 10 °C/min under air and nitrogen conditions, respectively. Differential scanning calorimetry (DSC) was conducted with a Netzsch STA 449C, heating from R.T. to 250 °C at a heating rate of 10 °C/min under nitrogen atmosphere. The mass of each sample was approximately 4-10 mg.

The limiting oxygen index (LOI) was determined with a JF-3 type instrument (Jiangning, China) with specimen dimension were 100 mm × 6 mm × 4 mm. The percentage of O_2 in the O_2/N_2 mixture was taken as the LOI which was just sufficient to sustain the flame.

Three-point bending experiments were conducted on an electronic universal testing machines (AGS-X, Shimadzu, Japan). The crosshead speed was 1 mm/min and typical dimensions of the sample beams were 120 mm × 10 mm × 5 mm.

Conclusions

In summary, we have successfully prepared a novel flame-retardant (POSS-bisDOPO) *via* Kabachnik-Fields reaction. The surfactant like structure of this flame-retardant endows it with excellent self-assembly capability, thus significantly improve its dispersion uniformity in epoxy resin. The self-assembly of POSS-bisDOPO in epoxy resin could not only obviously enhance the flame retardancy, but also improve the mechanical properties. Optical photograph and SEM analyses illustrated that the POSS-bisDOPO was dispersed in nanoscale in EP matrix. With 20 wt% loading of POSS-bisDOPO, the samples still had good transparency, and the LOI value increased from 25.4% to 34.5%. From the analysis of three-point bending test, with increasing loads the flexural strength increased first and then decreased. A hierarchical structure can be observed from the char with a smooth and compact inner layer, and an intumescent and multi-porous layer on the

outside. As a result that this char layer could protect the inner polymer matrix from further burning. And FT-IR spectra indicated the protective layer mainly contained Si-O-Si and aromatic structures. This surfactant like retardant might be a potential candidate as a new halogen free additives with high mechanical performance that extended to other thermosetting resin systems.

Acknowledgements

The financial support offered by National Natural Science Foundation of China (51373142, U1205113, 51273164), Scientific and Technological Innovation Platform of Fujian Province (2014H2006), Scientific and Technical Project of Fujian Province of China (2013H6019).

Notes and references

1. Y. Nakamura, M. Yamaguchi, M. Okubo and T. Matsumoto, *J. Appl. Polym. Sci.* , 1992, 45, 1281-1289.
2. L. Chen, S. Chai, K. Liu, N. Ning, J. Gao, Q. Liu, F. Chen and Q. Fu, *ACS Appl. Mat. Interfaces* 2012, 4, 4398-4404.
3. J. Wan, C. Li, Z.-Y. Bu, C.-J. Xu, B.-G. Li and H. Fan, *Chem. Eng. J.* , 2012, 188, 160-172.
4. C. Martin, G. Lligadas, J. Ronda, M. Galia and V. Cadiz, *J. Polym. Sci., Part A: Polym. Chem.* , 2006, 44, 6332-6344.
5. E. Franchini, J. Galy, J.-F. Gérard, D. Tabuani and A. Medici, *Polym. Degrad. Stab.* , 2009, 94, 1728-1736.
6. L. A. Mercado, M. Galià and J. A. Reina, *Polym. Degrad. Stab.* , 2006, 91, 2588-2594.
7. C. Li, J. Wan, E. N. Kalali, H. Fan and D.-Y. Wang, *J. Mater. Chem. A*, 2015, 3, 3471-3479.
8. J. Liu, J. Tang, X. Wang and D. Wu, *RSC Adv.*, 2012, 2, 5789.
9. K. A. Salmeia and S. Gaan, *Polym. Degrad. Stab.* , 2014, 113, 119-134.
10. I.-D. Carja, D. Serbezeanu, T. Vlad-Bubulac, C. Hamciuc, A. Coroaba, G. Lisa, C. G. López, M. F. Soriano, V. F. Pérez and M. D. Romero Sánchez, *J. Mater. Chem. A*, 2014, 2, 16230-16241.
11. W. Zhang, X. Li and R. Yang, *Polym. Degrad. Stab.* , 2011, 96, 2167-2173.
12. P. Chao, Y. Li, X. Gu, D. Han, X. Jia, M. Wang, T. Zhou and T. Wang, *Polym. Chem.*, 2015, 6, 2977-2985.
13. S. Song, J. Ma, K. Cao, G. Chang, Y. Huang and J. Yang, *Polym. Degrad. Stab.* , 2014, 99, 43-52.
14. C.-L. Chiang, R.-C. Chang and Y.-C. Chiu, *Thermochim. Acta* 2007, 453, 97-104.
15. G. Song, X. Li, Q. Jiang, J. Mu and Z. Jiang, *RSC Adv.*, 2015, 5, 11980-11988.
16. W. Zhang, X. He, T. Song, Q. Jiao and R. Yang, *Polym. Degrad. Stab.* , 2015, 112, 43-51.
17. W. Zhang, X. Li and R. Yang, *Polym. Degrad. Stab.* , 2012, 97, 1314-1324.
18. R. A. Cherkasov and V. I. Galkin, *Russ. Chem. Rev.* , 1998, 67, 857-882.
19. Y. Zhang, Y. Zhao, B. Yang, C. Zhu, Y. Wei and L. Tao, *Polym. Chem.*, 2014, 5, 1857-1862.
20. L. Valentini, S. B. Bon, O. Monticelli and J. M. Kenny, *J. Mater. Chem.* , 2012, 22, 6213-6217.
21. F. Carniato, E. Boccaleri and L. Marchese, *Dalton Trans.* , 2008, DOI: 10.1039/b715664m, 36-39.
22. O. Mauerer, *Polym. Degrad. Stab.* , 2005, 88, 70-73.
23. A. Schäfer, S. Seibold, O. Walter and M. Döring, *Polym. Degrad. Stab.* , 2008, 93, 557-560.
24. C. G. Robertson and C. M. Roland, *Rubber Chem. Technol.* , 2008, 81, 506-522.
25. H. Wang, Y. Zhang, L. Zhu, Z. Du, B. Zhang and Y. Zhang, *Thermochim. Acta* 2011, 521, 18-25.
26. X. Zhang, Q. He, H. Gu, H. A. Colorado, S. Wei and Z. Guo, *ACS Appl. Mat. Interfaces* 2013, 5, 898-910.
27. X. Wang, Y. Hu, L. Song, W. Xing, H. Lu, P. Lv and G. Jie, *Polymer*, 2010, 51, 2435-2445.
28. K. Wu, L. Song, Y. Hu, H. Lu, B. K. Kandola and E. Kandare, *Prog. Org. Coat.* , 2009, 65, 490-497.
29. J.-Y. Shieh and C.-S. Wang, *Polymer*, 2001, 42, 7617-7625.
30. X. Wang, Y. Hu, L. Song, H. Yang, W. Xing and H. Lu, *Prog. Org. Coat.* , 2011, 71, 72-82.
31. B. Yu, Y. Shi, B. Yuan, S. Qiu, W. Xing, W. Hu, L. Song, S. Lo and Y. Hu, *J. Mater. Chem. A*, 2015, 3, 8034-8044.
32. B. Yu, X. Wang, X. Qian, W. Xing, H. Yang, L. Ma, Y. Lin, S. Jiang, L. Song, Y. Hu and S. Lo, *RSC Adv.*, 2014, 4, 31782.
33. B. Yu, Y. Tao, L. Liu, Y. Shi, H. Yang, G. Jie, S. Lo, Q. Tai, L. Song and Y. Hu, *RSC Adv.*, 2015, 5, 75254-75262.

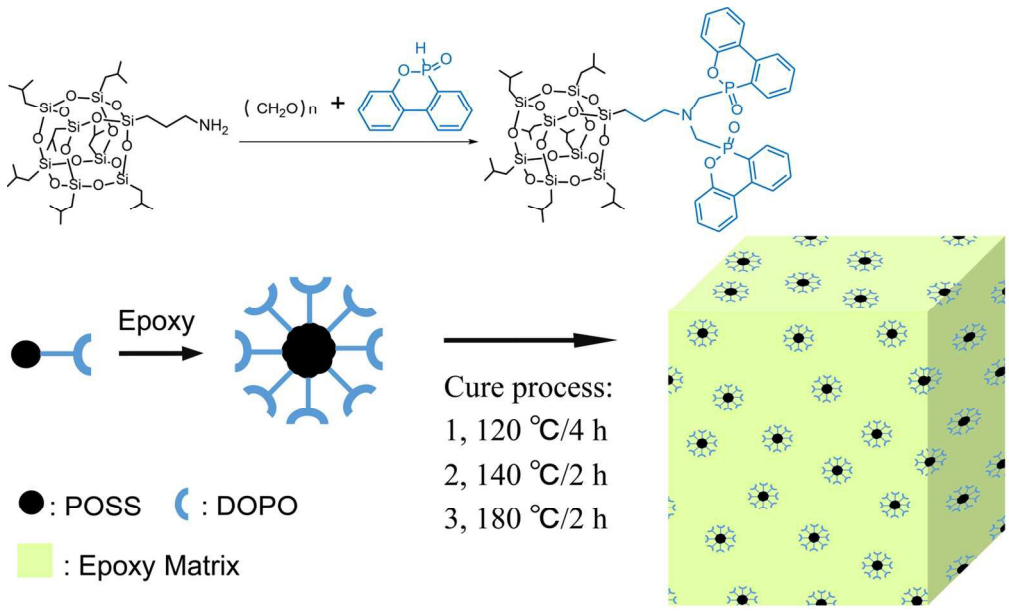

68x41mm (600 x 600 DPI)